Progress In Electromagnetics Research B, Vol. 6, 337–360, 2008

A STABLE MARCHING-ON-IN-TIME SCHEME FOR WIRE SCATTERERS USING A NEWMARK-BETA FORMULATION

S. E. Bayer

University of Kocaeli
Mechatronic Engineering Department
Veziroglu Campus, İzmit, Kocaeli, Turkey

A. A. Ergin

Gebze Institute of Technology
Electronic Engineering Department
Çayırova Campus, P.K.: 141,41400 Çayrova, Gebze/Kocaeli, Turkey

Abstract—The aim of this work is to increase the instability of the marching-on-in-time (MOT) method that is used in the analysis of wide-band electromagnetic pulse scattering from structures made of thin wires. The stability problem has been identified with the advent of the MOT method in 1991, and although several improvements have been suggested to overcome this difficulty no exact solution has been found [1]. In this thesis two methods (the Newmark-Beta formulation and the analytic integration) to suppress the instabilities of the MOT algorithm for thin wire scatterers have been proposed and their effects on the stability have been inspected. The results are compared with the results obtained with time domain method of moments (MOM) [2] and it is observed that the results are both stable and accurate. It is shown how the stability is changed by a determined β parameter. Also, Newmark-Beta formulation results for selected different types of structures such as dipole antenna illuminated by a Gaussian pulse given in [3], three pole structure given in [4], loop antenna given in [3] has been shown.

1. INTRODUCTION

Nowadays, there is a growing interest in the study of radiation and propagation of transient electromagnetic waves. Numerical methods have very important roles for the analysis of transient electromagnetic scattering problems and may involve both frequency-domain (FD) solutions together with inverse discrete Fourier transform (IDFT) technique to convert the results to time domain or time-domain (TD) solutions by formulating the problem directly in the time-domain using a time-marching algorithm. Most popular time-domain techniques are the method of finite difference in time domain (FDTD) [5] and the method of marching-on-in-time (MOT) [6, 7].

This study aims to increase the stability of the MOT method which was developed to examine scattering of wide-band electromagnetic pulses from objects. In the past, various solutions were suggested to increase the stability of the MOT method such as time or space averaging methods [7–10], good choice of temporal basis functions [11], and the use of combined-field integral equation [1]. However, the solutions in question are either applicable for analysis of scattering from surfaces (for example, [1]) or provide stability by employing artificial signal processing techniques [7–10]. As a result, literature does not contain a special stability analysis and solution suggestion developed for the MOT methods solving the problem of scattering from thin wires.

This study suggests two basic solutions to increase the stability in analysis of scattering from wires. The first solution is the Newmark-Beta formulation which was used in general for the time-domain finite element method (FEM) [12]. This method calculates the derivatives of the terms approximately by using finite differences and uses an independent beta (β) parameter to increase the stability. The second solution examines the contribution of analytic evaluation of some of the integrals, which had been considered in numerical terms to date for the MOT method, to the stability. Numeric errors have been suggested to be one of the reasons of instability in the MOT method [8]. Here the basic hypothesis is that, the integral results calculated analytically will eliminate some of the numeric errors and will contribute to the stability.

2. THE ELECTRIC FIELD INTEGRAL EQUATION (EFIE)

The electric field integral equation (EFIE) is based on the condition that the total tangential electric field on a perfect electric conducting

(PEC) scatterer surface is equal to zero. Therefore, we have

$$\frac{\partial \boldsymbol{E}_t^i}{\partial t} = \left[\frac{\partial^2 \boldsymbol{A}}{\partial t^2} + \frac{\partial}{\partial t}\nabla\phi\right]_t \tag{1}$$

where $\boldsymbol{A}$ and ϕ are the magnetic vector and scalar electric potentials, respectively, and $\boldsymbol{E}^i$ denotes the incident electric field. The subscript 't' denotes the tangential components to wire surface. The magnetic vector potential $\boldsymbol{A}$ and scalar potential ϕ are in the retarded time integral form and are mathematically represented by

$$\boldsymbol{A}(\boldsymbol{r},t) = \mu \int\limits_v \frac{\boldsymbol{J}(\boldsymbol{r},t-R/c)}{4\pi R}dv' \qquad \phi(\boldsymbol{r},t) = \frac{1}{\varepsilon}\int\limits_v \frac{\rho(\boldsymbol{r},t-R/c)}{4\pi R}dv \tag{2}$$

where $R = |\boldsymbol{r} - \boldsymbol{r'}|$ represents the distance between the observation point $\boldsymbol{r}$ and source point $\boldsymbol{r'}, \rho$ is the charge density, $\boldsymbol{J}$ is the current density, c is the velocity of propagation of electromagnetic wave in the space, μ and ε are the permeability and permittivity of free space, respectively. $t - R/c$ represents the retarded time. In Eq. (1), the incident field $\boldsymbol{E}_t^i$ is known and induced current density on the scatterer $\boldsymbol{J}(\boldsymbol{r}, t - R/c)$ is not known, but it is wanted to be found.

3. SOLUTION OF EFIE FOR THIN-WIRES BY CLASSICAL MOT

In this section the solution of the EFIE for thin wires by the classical MOT method will be outlined.

3.1. Basis Function

When conductors are thin wires ($a \ll \lambda$), the current is assumed to flow only in the wire axis direction $\hat{\ell}$ and only along the wire axis. Hence, the unknown current density can be expressed as $\boldsymbol{J}(\boldsymbol{r},t) = \boldsymbol{J}(\ell,t) = \hat{\ell}(\ell)I(\ell,t)$ by using thin wire approximation.

Current density in terms of N spatial basis functions $\boldsymbol{f}_n(\ell)$, and temporal basis functions $T_i(t)$ is:

$$\boldsymbol{J}(\ell,t) = \sum_{n=1}^{N} I_n(t)\boldsymbol{f}_n(\ell) = \sum_{n=1}^{N}\sum_i I_{n,i}T_i(t)\boldsymbol{f}_n(\ell) \tag{3}$$

Here, $I_{n,i}$ are the unknown coefficients, $T_i(t)$ is time basis function and it can be expressed as $T_i(t) = T(t - i\Delta t)$ where it is assumed time

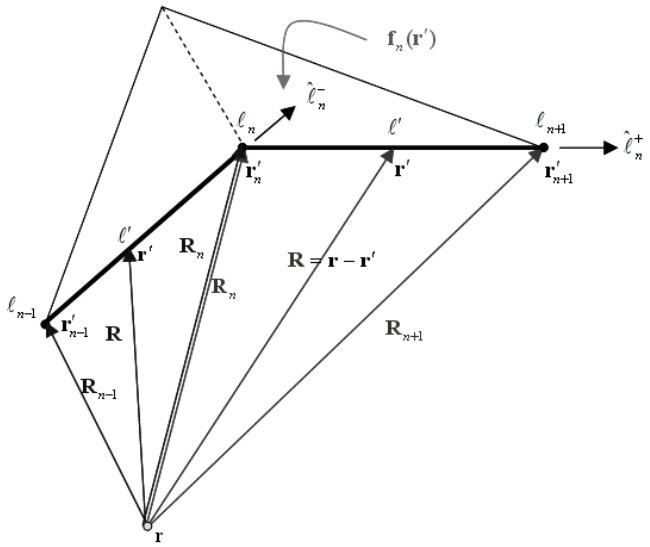

Figure 1. Definition of the basis function.

interval is divided into Δt equal time steps and $T(t)$ is a quadratic function [13]. The subscript 'i' denotes the current on the ith time step is related with basis functions $T(t - i\Delta t)$. $\boldsymbol{f}_n(\ell)$ is a linear basis function [14], the parameters related to the spatial basis function $\boldsymbol{f}_n(\ell')$ are shown in Fig. 1 and its mathematical expression can be given as

$$\boldsymbol{f}_n(\ell') = \begin{cases} \dfrac{\ell' - \ell_{n-1}}{s_n^-}\hat{\ell}_n^- & \ell' \in S_n^- \\ \dfrac{\ell_{n+1} + \ell'}{s_n^+}\hat{\ell}_n^+ & \ell' \in S_n^+ \end{cases} \quad ; \quad n \in \{1, \ldots, N\} \tag{4}$$

Here, ℓ_n means nth node's coordinate in term of ℓ parameter and $s_n^{\pm} = |\ell_{n+1} - \ell_n|$. Also, s_n^- is wire segment between $[\ell_{n-1}, \ell_n]$ points and s_n^+ is wire segment between $[\ell_n, \ell_{n+1}]$ points. Eq. (4) can be written as

$$\boldsymbol{f}_n(\ell') = \left\{ \pm \frac{\ell_{n\pm1} - \ell}{s_n^{\pm}}\hat{\ell}_n^{\pm} \qquad \ell_n \lesseqgtr \ell \lesseqgtr \ell_{n\pm1} \right. \tag{5}$$

For the thin wire case, the EFIE can be written in the form of

$$\partial_t \boldsymbol{E}_t^i(\ell, t) = \left[\partial_t^2 \boldsymbol{A}(\ell, t) + \nabla \partial_t \phi(\ell, t)\right]_t \tag{6}$$

where ∂_t denotes $\partial/\partial t$. After substituting Eq. (3) in (6), so we need to solve this integro-differential equation.

3.2. Testing Procedure

If we apply spatial Galerkin testing at time $t = t_j$ to Eq. (6), the result is

$$\underbrace{\left\langle \boldsymbol{f}_m(\ell), \partial_t \boldsymbol{E}^i(\ell,t) \right\rangle \Big|_{t=t_j}}_{E_{mj}} = \partial_t^2 \underbrace{\langle \boldsymbol{f}_m(\ell), \boldsymbol{A}(\ell,t) \rangle \Big|_{t=t_j}}_{\psi_{mj}} + \underbrace{\langle \boldsymbol{f}_m(\ell), \nabla \partial_t \phi(\ell,t) \rangle \Big|_{t=t_j}}_{varphi_{mj}}; \; m \in \{1,\ldots,N\} \quad (7)$$

where $\langle f, g \rangle$ inner product is $\langle f, g \rangle = \int f(\ell) g(\ell) d\ell$. Eq. (7) can be written as

$$E_{m,j} = \partial_t^2 \psi_{m,j} + \varphi_{m,j} \quad (8)$$

Since there are N number of basic functions, different $m \in \{1,\ldots,N\}$ values can be used for Eq. (7) in order to write an equation indicating N number of numeric parities. Second order derivative in Eq. (8) can be implemented with the finite difference method and Eq. (8) can be written in the form

$$E_{m,j} \cong \frac{\psi_{m,j+1} - 2\psi_{m,j} + \psi_{m,j-1}}{\Delta t^2} + \varphi_{m,j} \quad (9)$$

approximately. In the inner product expression shown as $\psi_{m,j}$ in Eq. (7), can be written as

$$\psi_{m,p} = \langle \boldsymbol{f}_m(\ell), \boldsymbol{A}(\ell,t) \rangle \Big|_{t=t_p} = \int_{S_m} \boldsymbol{f}_m(\ell) \boldsymbol{A}(\ell, t_p) d\ell \quad (10)$$

can be expanded by using Eqs. (2), (3) and the result can be shown as

$$\psi_{m,p} = \mu \int_{S_m} \boldsymbol{f}_m(\ell) \cdot \int_S \frac{\boldsymbol{J}(\ell', t_p - R/c)}{4\pi R} d\ell' d\ell = \frac{\mu}{4\pi} \sum_{n=1}^{N} \sum_i I_{n,i} \underbrace{\int_{S_m} \boldsymbol{f}_m(\ell) \cdot \int_{S_n} \boldsymbol{f}_n(\ell') \frac{T_i(t_p - R/c)}{R} d\ell' d\ell}_{Z^{\psi}_{mn,p-i}} \quad (11)$$

And Eq. (11) can be written in matrix form as:

$$\overline{\psi}_p = \frac{\mu}{4\pi} \sum_i \overline{\overline{Z}}^{\psi}_{p-i} \overline{I}_i \quad (12)$$

In Eq. (11), the term $Z_{mn,p-i}$ can be interpreted as the "potential created by the nth basis function radiating at time i on the mth test function at time p". Similarly, the inner product expression shown as $\varphi_{m,j}$ in Eq. (7) can be written in the similar form:

$$\begin{aligned}\varphi_{m,p} &= \langle \boldsymbol{f}_m(\ell), \nabla\partial_t\phi(\ell,t)\rangle\Big|_{t=t_p} = \int\limits_{S_m} \boldsymbol{f}_m(\ell)\nabla\partial_t\phi(\ell,t_p)d\ell \\ &= \int\limits_{S_m} \nabla\cdot[\boldsymbol{f}_m(\ell)\partial_t\phi(\ell,t_p)]\,d\ell - \int\limits_{S_m}[\nabla\cdot\boldsymbol{f}_m(\ell)]\,\partial_t\phi(\ell,t_p)d\ell \quad (13)\end{aligned}$$

Benefiting from the fundamental theorem of calculus, it can be shown the expression $\int_{S_m}\nabla\cdot[\boldsymbol{f}_m(\ell)\partial_t\phi(\ell,t_p)]d\ell$ in Eq. (13) is equal to zero. Then Eq. (13) can be written in the form of

$$\begin{aligned}\varphi_{m,p} &= -\int\limits_{S_m}[\nabla\cdot\boldsymbol{f}_m(\ell)]\partial_t\phi(\ell,t_p)d\ell \\ &= \frac{1}{4\pi\varepsilon}\int\limits_{S_m}[\nabla\cdot\boldsymbol{f}_m(\ell)]\int\limits_{S}\frac{\nabla\cdot\boldsymbol{J}(\ell',t_p-R/c)}{R}d\ell' d\ell \\ &= \frac{\mu}{4\pi}\sum_{n=1}^{N}\sum_i I_{n,i}c^2\underbrace{\int\limits_{S_m}[\nabla\cdot\boldsymbol{f}_m(\ell)]\int\limits_{S_n}[\nabla\cdot\boldsymbol{f}_n(\ell')]\frac{T_i(t_p-R/c)}{R}d\ell' d\ell}_{Z^{\varphi}_{mn,p-i}}\end{aligned} \quad (14)$$

Eq. (14) can be written in matrix form as:

$$\overline{\varphi}_p = \frac{\mu}{4\pi}\sum_i \overline{\overline{Z}}^{\varphi}_{p-i}\overline{I}_i \quad (15)$$

In Eq. (12) and Eq. (15), summation of $\sum\limits_i$ must be started from "zero" ($i=0$) because it is assumed that the electric field illuminates the wire at the time instant $t=0$.

When Eq. (10) and (14) are added into Eq. (9), it can be written in matrix form as:

$$\Delta t^2\overline{E}_j = \overline{\psi}_{j+1} - 2\overline{\psi}_j + \overline{\psi}_{j-1} + \Delta t^2\overline{\varphi}_j \quad (16)$$

As the value of the current at the $(j+1)$st time step shown in Eq. (16) is drawn, the current values are calculated by marching on step by step in time. Since this method reaches a conclusion by stepping in time,

it is known as "Marching-on-in-Time". The current density which is induced on the wire can be obtained by pulling out as:

$$\overline{I}_{j+1} = \left[\overline{\overline{Z}}_0^{\psi}\right]^{-1} \left[\frac{4\pi}{\mu}\Delta t^2 \overline{E}_j - \sum_{i=0}^{j-1} \overline{\overline{\Lambda}}_{j-i}\overline{I}_i - \overline{\overline{\Lambda}}_0 \overline{I}_j\right] \tag{17}$$

and the current density term which occurs at $(j+1)$st time step can be calculated marching in the time step by step. Here, $\overline{\overline{\Lambda}}_{j-i}$ and $\overline{\overline{\Lambda}}_0$ can be defined as

$$\begin{aligned} \overline{\overline{\Lambda}}_{j-i} &= \overline{\overline{Z}}_{j-i+1}^{\psi} - 2\overline{\overline{Z}}_{j-i}^{\psi} + \overline{\overline{Z}}_{j-i-1}^{\psi} + \Delta t^2 \overline{\overline{Z}}_{j-1}^{\varphi} \\ \overline{\overline{\Lambda}}_0 &= \overline{\overline{Z}}_1^{\psi} - 2\overline{\overline{Z}}_0^{\psi} + \Delta t^2 \overline{\overline{Z}}_0^{\varphi} \end{aligned} \tag{18}$$

For instance, for the first time step ($j = 0$) current value I_1 can be calculated as

$$\overline{I}_1 = \left[\overline{\overline{Z}}_0^{\psi}\right]^{-1} \left[\frac{4\pi}{\mu}\Delta t^2 \overline{E}_0\right] \tag{19}$$

and for the time step $j = 1$ current value I_2 can be calculated as

$$\overline{I}_2 = \left[\overline{\overline{Z}}_0^{\psi}\right]^{-1} \left[\frac{4\pi}{\mu}\Delta t^2 \overline{E}_1 - \overline{\overline{\Lambda}}_1 \overline{I}_0 - \overline{\overline{\Lambda}}_0 \overline{I}_1\right] \tag{20}$$

In the classic marching-on-in-time method, the integrals shown in Eq. (11) and Eq. (14) are evaluated numerically. It has been observed in the studies we conducted that evaluating these integrals by employing the 7-point Gauss-Legendre method over triangular patches is sufficient.

4. SOLUTION OF EFIE FOR THIN-WIRES BY NEWMARK-BETA FORMULATION (B-MOT)

It will be shown in Section 6 that the solutions arrived by employing the classic MOT method described in the previous section are instable. Such instabilities have prevented the MOT method from being used in a wide scale. Although many studies were conducted to overcome these instabilities in surface scattering problems, the number of studies conducted on problems of scattering from wire structures is almost nil. It is known that similar instabilities were also observed in the time-domain finite element method and that the Newmark-Beta formulation was suggested to solve them [12]. Newmark-Beta Formulation can be

given as

$$\frac{d^2v}{dt^2} = \frac{1}{\Delta t^2}[v(n+1) - 2v(n) + v(n+1)] \tag{21}$$

$$\frac{dv}{dt} = \frac{1}{2\Delta t}[v(n+1) - v(n-1)] \tag{22}$$

$$v = \beta v(n+1) + (1-2\beta)v(n) + \beta v(n-1) \tag{23}$$

In Eqs. (21)–(23), expression of $v(n)$ is discrete form of $v(t)$ function and it can be written as $v(n) = v(n\Delta t)$. β is a free parameter that effects stability.

This section examines whether or not the use of the Newmark-Beta formulation in the MOT method will also provide stability. In Section 3.2, second order derivation in Eq. (8) was implemented with the finite difference method which is identical with Eq. (21). Additionally, by using Eq. (23), $\varphi_{m,j}$ term in Eq. (9) can be expanded as

$$E_{m,j} \cong \frac{\psi_{m,j+1} - 2\psi_{m,j} + \psi_{m,j-1}}{\Delta t^2} + \beta\varphi_{m,j+1} + (1-2\beta)\varphi_{m,j} + \beta\varphi_{m,j-1} \tag{24}$$

approximately. This equation can be expressed in matrix form as follows:

$$\Delta t^2 \overline{E}_j = \overline{\psi}_{j+1} - 2\overline{\psi}_j + \overline{\psi}_{j-1} + \Delta t^2 \left[\beta\overline{\varphi}_{j+1} + (1-2\beta)\overline{\varphi}_j + \beta\overline{\varphi}_{j-1}\right] \tag{25}$$

If it is considered in this expression that $\beta = 0$, it will be understood that the definition given in Eq. (9) is reached. In other words, the classic formulation is a special case of the Newmark-Beta formulation. Using Eq. (25), the current values at $(j+1)^{st}$ time step is calculated by employing the marching-on-in-time method in the same way as the classic formulation. Due to the use of the β parameter, this method will be referred to as "B-MOT" henceforth.

As it will be evident in Section 6, the use of B-MOT formulation outlined here does produce stable results for judiciously chosen β values. However, it is observed that the results are not accurate. Hence, the following measures are taken to assure accuracy. In this method, integrals are also evaluated numerically.

5. SOLUTION OF EFIE WITH ANALYTIC EVALUATION OF POTENTIAL INTEGRALS

In the classic and B-MOT formulations, the integrals in $\psi_{m,p}$ and $\varphi_{m,p}$ were calculated numerically. Analytic results of the relevant integrals were expressed and used in the frequency domain in the past.

However, this study uses a new formulation by calculating the analytic results directly in the time domain by taking into account the currents' variation in time, too.

The term $\boldsymbol{J}(\ell, t_p - R/c)$ included in Eq. (10) can be expressed as the $\boldsymbol{J}(\ell, t)$ current density's convolution with the Dirac delta function as $\boldsymbol{J}(\ell, t) * \delta(t - R/c)$. Thus, the term $\boldsymbol{J}(\ell, t_p - R/c)$ can be written in the form of

$$\boldsymbol{J}_n(\ell, t - R/c) = \boldsymbol{J}_n(\ell, t) * \delta\left(t - \frac{R}{c}\right) = \int \boldsymbol{J}_n(\ell, t - t')\delta\left(t' - \frac{R}{c}\right) dt' \tag{26}$$

Current density term in Eq. (26) can be expanded in terms of N spatial basis functions $\boldsymbol{f}_n(\ell)$, and temporal basis functions $T_i(t)$ as

$$\boldsymbol{J}_n(\ell, t - R/c) = \sum_{n=1}^{N} \sum_{i} I_{n,i} \int_{-\infty}^{\infty} T_i(t - t')\delta\left(t' - \frac{R}{c}\right) \boldsymbol{f}_n(\ell) dt' \tag{27}$$

Hence Eq. (10) can be rearranged as follows:

$$\psi_{m,p} = \int_{S_m} \boldsymbol{f}_m(\ell) \cdot \mu \int_{S} \frac{\boldsymbol{J}(\ell', t_p - R/c)}{4\pi R} d\ell' d\ell \tag{28}$$

$$= \frac{\mu}{4\pi} \sum_{n=1}^{N} \sum_{i} I_{n,i} \underbrace{\int_{S_m} \boldsymbol{f}_m(\ell) \cdot \underbrace{\int_{-\infty}^{\infty} T_i(t_p - t') \underbrace{\int_{S_n} \boldsymbol{f}_n(\ell') \frac{\delta\left(t' - \frac{R}{c}\right)}{R} d\ell'}_{\boldsymbol{h}_n^{\psi}(\ell, t')} dt'}_{\boldsymbol{V}_n^{\varphi}(\ell, t_p - t_i)} d\ell}_{Z_{mn,p-i}^{\varphi}}$$

Similarly, Eq. (14) can be arranged as follows:

$$\varphi_{m,p} = \tag{29}$$

$$\frac{\mu}{4\pi} \sum_{n=1}^{N} \sum_{i} I_{n,i} c^2 \underbrace{\int_{S_m} [\nabla \cdot \boldsymbol{f}_m(\ell)] \underbrace{\int_{-\infty}^{\infty} T_i(t_p - t') \underbrace{\int_{S_n} [\nabla \cdot \boldsymbol{f}_n(\ell')] \frac{\delta\left(t' - \frac{R}{c}\right)}{R} d\ell'}_{h_n^{\psi}(\ell, t')} dt'}_{V_n^{\varphi}(\ell, t_p - t_i)} d\ell}_{Z_{mn,p-i}^{\varphi}}$$

The analytic expressions of $\boldsymbol{h}_n(\ell, t')$ and $\boldsymbol{V}_n(\ell, t_p - t_i)$ will be given in Sections 5.1 and 5.2. Currents can be calculated by calculating the integrals included in Eq. (28) and Eq. (29) and adding them into Eq. (25). Comparison of the currents calculated by using the B-MOT and analytic formulations presented in this section (and henceforth referred to as A-MOT) with those calculated by employing the time domain method of moments (MOM) [2] has been given in Section 6. It is observed that the results obtained with A-MOT are stable and accurate.

5.1. Calculation of $\psi_{m,p}$ Expression Anatically

Integration of $\boldsymbol{h}_n(\ell, t')$ can be written in terms of "+" and "−" egments as shown in Eq. (5) can be written as

$$\begin{aligned}
\boldsymbol{h}_n^{\psi\pm}(\ell, t') &= \int\limits_{S_n^{\pm}} \boldsymbol{f}_n(\ell') \frac{\delta\left(t' - \dfrac{R}{c}\right)}{R} d\ell' \\
&= \int\limits_{\ell_n}^{\ell_{n\pm1}} \frac{\ell_{n\pm1} - \ell'}{s_n^{\pm}} \hat{\ell}_n^{\pm} \frac{\delta\left(t' - \dfrac{R}{c}\right)}{R} d\ell' \\
&= c \int\limits_{\ell_n}^{\ell_{n\pm1}} \frac{\ell_{n\pm1} - \ell'}{s_n^{\pm}} \hat{\ell}_n^{\pm} \frac{\delta(ct' - R)}{R} d\ell'
\end{aligned} \tag{30}$$

At last step of Eq. (30), the rule which has been given below is used.

$$\int\limits_S \delta\left(t - \frac{|\boldsymbol{r}|}{c}\right) d\boldsymbol{r} = c \int\limits_S \delta(ct - |\boldsymbol{r}|) d\boldsymbol{r} \tag{31}$$

In Eq. (30), R has been defined as

$$R = \sqrt{(\ell')^2 + \left(d_n^{\pm}\right)^2} \tag{32}$$

As its known square root function has double value, so ℓ' can be defined as

$$\ell' = \chi \sqrt{|\boldsymbol{r}' - \boldsymbol{r}|^2 - \left(d_n^{\pm}\right)^2}; \qquad \chi = \begin{cases} -1 & \hat{\ell} \cdot (\boldsymbol{r}' - \boldsymbol{r}) < 0 \\ 1 & \hat{\ell} \cdot (\boldsymbol{r}' - \boldsymbol{r}) > 0 \end{cases} \tag{33}$$

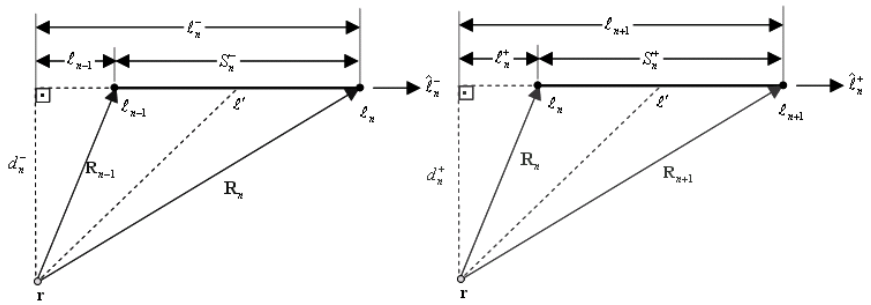

Figure 2. Definition of the basis function's two segments.

Here, $d_n^{\pm}$, as shown in Figure 2, is perpendicular distance between observation point and the wire segment and it can be defined as

$$d_n^{\pm} = \sqrt{|\boldsymbol{R}|^2 - |\boldsymbol{R} \cdot \hat{\ell}^{\pm}|^2} \tag{34}$$

By exchanging integration variable ℓ' with $R, d\ell'$ can be written as

$$d\ell' = \frac{RdR}{\chi\sqrt{R^2 - \left(d_n^{\pm}\right)^2}} \tag{35}$$

By using Eq. (35), Eq. (30) can be written as

$$\boldsymbol{h}_n^{\psi\pm}(\ell, t') = c\hat{\ell}_n^{\pm} \int_{R_n}^{R_{n\pm1}} \frac{\ell_{n\pm1} - \chi\sqrt{R^2 - \left(d_n^{\pm}\right)^2}}{s_n^{\pm}} \frac{\delta(ct' - R)}{R} \frac{RdR}{\chi\sqrt{R^2 - \left(d_n^{\pm}\right)^2}} \tag{36}$$

By using the rule given in Eq. (37)

$$\int_S \delta(t - \tau)\boldsymbol{f}(\tau)d\tau = \boldsymbol{f}(t) \qquad t \in S \tag{37}$$

Eq. (36) can be written as

$$\boldsymbol{h}_n^{\psi\pm}(\ell, t') = \hat{\ell}_n^{\pm} \left[\chi \frac{\ell_{n\pm1}}{s_n^{\pm}} \frac{1}{\sqrt{(t')^2 - \left(\dfrac{d_n^{\pm}}{c}\right)^2}} - \frac{c}{s_n^{\pm}} \right]; \ \frac{R_n}{c} \lesseqgtr t' \lesseqgtr \frac{R_{n\pm1}}{c} \tag{38}$$

By using Table 1, Eq. (38) can be defined as

$$\boldsymbol{h}_n^{\psi\pm}(\ell,t') = \hat{\ell}_n \left[\frac{C_1}{\sqrt{(t')^2-C_2^2}} - C_3\right]; \quad \frac{R_n}{c} \lesseqgtr t' \lesseqgtr \frac{R_{n\pm1}}{c} \tag{39}$$

In Eq. (28), $\boldsymbol{V}_n(\ell, t_p - t_i)$ expression defined as

$$\begin{aligned}\boldsymbol{V}_n^{\psi}(\ell,t_p-t_i) &= \int_{-\infty}^{\infty} T_i(t_p-t')h_n^{\psi}(\ell,t')dt' \\ &= \int_{-\infty}^{\infty} T_i(t_p-t')h_n^{\psi+}(\ell,t')dt' + \int_{-\infty}^{\infty} T_i(t_p-t')h_n^{\psi-}(\ell,t')dt'\end{aligned} \tag{40}$$

In Eq. (40), $T_i(t_p - t')$ can be written as $T(t_p - t_i - t') = T(t_q - t')$ and according to [8] temporal basis funciton $T(t_q - t')$ can be given as

$$T(t_q-t') = \begin{cases} \dfrac{(t_q-t')^2}{2\Delta t^2} + \dfrac{3(t_q-t')}{2\Delta t} + 1 & ; \quad t_q \le t' \le t_q + \Delta t \\ -\dfrac{(t_q-t')^2}{\Delta t^2} + 1 & ; \quad t_q - \Delta t \le t' \le t_q \\ \dfrac{(t_q-t')^2}{2\Delta t^2} - \dfrac{3(t_q-t')}{2\Delta t} + 1 & ; \quad t_q - 2\Delta t \le t' \le t_q - \Delta t \end{cases} \tag{41}$$

or

$$T(t_q-t') = e(t')^2 + ft' + g \tag{42}$$

In Eq. (42), e, f and g denotes constant coefficients.

By substituting Eq. (39) and Eq. (42), Eq. (40) can be written as

$$\begin{aligned}\boldsymbol{V}_n^{\psi}(\ell,t_p-t_i) &= \hat{\ell}_n \int_{\frac{R_n}{c}}^{\frac{R_{n+1}}{c}} (e(t')^2 + ft' + g)\left[\frac{C_1}{\sqrt{(t')^2-C_2^2}} - C_3\right]dt' \\ &+\hat{\ell}_n \int_{\frac{R_{n-1}}{c}}^{\frac{R_n}{c}} (e(t')^2 + ft' + g)\left[\frac{C_1}{\sqrt{(t')^2-C_2^2}} - C_3\right]dt'\end{aligned} \tag{43}$$

This integration can be calculated by using Table 2. Then, by calculating

$$Z_{mn,p-i}^{\psi} = \int_{S_m} \boldsymbol{f}_m(\ell)\boldsymbol{V}_n^{\psi}(\ell,t_p-t_i)d\ell \tag{44}$$

Table 1. Coefficients for Eq. (39).

	C_1	C_2	C_3	$\hat{\ell}_n$	Limits
$\mathbf{h}_n^+$	$\chi\frac{\ell_{n+1}}{\lvert\ell_{n+1}-\ell_n\rvert}$	$\frac{d_n^+}{c}$	$\frac{c}{\lvert\ell_{n+1}-\ell_n\rvert}$	$\hat{\ell}_n^+$	$t_n \rightarrow t_{n+1}$
$\mathbf{h}_n^-$	$\chi\frac{\ell_{n-1}}{\lvert\ell_{n-1}-\ell_n\rvert}$	$\frac{d_n^-}{c}$	$\frac{c}{\lvert\ell_{n+1}-\ell_n\rvert}$	$-\hat{\ell}_n^-$	$t_{n-1} \rightarrow t_n$

Table 2. Integration table.

$$\int \frac{dx}{\sqrt{x^2-a^2}} = \ln\left(x+\sqrt{x^2-a^2}\right)$$
$$\int \frac{xdx}{\sqrt{x^2-a^2}} = \sqrt{x^2-a^2}$$
$$\int \frac{x^2dx}{\sqrt{x^2-a^2}} = \frac{x\sqrt{x^2-a^2}}{2} + \frac{a^2}{2}\ln\left(x+\sqrt{x^2-a^2}\right)$$
$$\int \frac{x^3dx}{\sqrt{x^2-a^2}} = \frac{(x^2-a^2)^{3/2}}{3} + a^2\sqrt{x^2-a^2}$$

Here, integration can be calculated numerically as in Section 3. The $\psi_{m,p}$ term can be written in the matrix form as

$$\psi_{m,p} = \frac{\mu}{4\pi}\sum_{n=1}\sum_i I_{n,i} Z^{\psi}_{mn,p-i} \tag{45}$$

5.2. Calculation of $\varphi_{m,p}$ Expression Analytically

In Eq. (29), $h_n^{\varphi}(\ell, t')$ expression was given as

$$h_n^{\varphi}(\ell, t') = \int_{S_n} [\nabla \cdot \boldsymbol{f}_n(\ell')] \frac{\delta(t' - R/c)}{R} d\ell' \tag{46}$$

In Eq. (46), divergence term can be define as

$$\nabla \cdot \boldsymbol{f}_n(\ell') = \begin{cases} \dfrac{1}{s_n^-} & \ell' \in S_n^- \\ -\dfrac{1}{s_n^+} & \ell' \in S_n^+ \end{cases} \tag{47}$$

By using Eq. (47), Eq. (46) can be written as

$$h_n^{\varphi\pm}(\ell,t') = \underbrace{\int\limits_{S_n^-} \frac{1}{s_n^-}\frac{\delta(t'-R/c)}{R}d\ell'}_{h_n^{\varphi-}(\ell,t')} - \underbrace{\int\limits_{S_n^+} \frac{1}{s_n^+}\frac{\delta(t'-R/c)}{R}d\ell'}_{h_n^{\varphi+}(\ell,t')} \tag{48}$$

By using the rule given in Eq. (50), Eq. (48) can be re-arranged as

$$h_n^{\varphi\pm}(\ell,t') = c\int\limits_{\ell_{n-1}}^{\ell_n} \frac{1}{s_n^-}\frac{\delta(ct'-R)}{R}d\ell' - c\int\limits_{\ell_n}^{\ell_{n+1}} \frac{1}{s_n^+}\frac{\delta(ct'-R)}{R}d\ell' \tag{49}$$

$$\int\limits_S \delta\left(t-\frac{|\boldsymbol{r}|}{c}\right)d\boldsymbol{r} = c\int\limits_S \delta(ct-|\boldsymbol{r}|)d\boldsymbol{r} \tag{50}$$

By exchanging integration variable ℓ' with R, Eq. (49) can be written as

$$\begin{aligned} h_n^{\varphi\pm}(\ell,t') \;=\; & c\int\limits_{\ell_{n-1}}^{\ell_n} \frac{1}{s_n^-}\frac{\delta(ct'-R)}{\cancel{R}}\frac{\cancel{R}dR}{\chi\sqrt{R^2-\left(d_n^\pm\right)^2}} \\ & -c\int\limits_{\ell_n}^{\ell^{n+1}} \frac{1}{s_n^+}\frac{\delta(ct'-R)}{\cancel{R}}\frac{\cancel{R}\,dR}{\chi\sqrt{R^2-\left(d_n^\pm\right)^2}} \end{aligned} \tag{51}$$

By using the rule given in Eq. (37), Eq. (51) can be shown as

$$\begin{aligned} h_n^{\varphi\pm}(\ell,t') &= c\frac{1}{s_n^-}\frac{dR}{\chi\sqrt{ct'-\left(d_n^\pm\right)^2}} - c\frac{1}{s_n^+}\frac{dR}{\chi\sqrt{ct'-\left(d_n^\pm\right)^2}};\;\; R_n \lesseqgtr ct' \lesseqgtr R_{n\pm1} \\ &= \mp c\frac{1}{s_n^\pm}\frac{dR}{\chi\sqrt{ct'-\left(d_n^\pm\right)^2}}; \quad R_n \lesseqgtr ct' \lesseqgtr R_{n\pm1} \end{aligned} \tag{52}$$

Table 3. Coeffients used in $\varphi_{m,p}$ integration.

	C_1	C_2	Limits
$h_n^{\varphi+}(\ell,t')$	$-\frac{1}{s_n^+}$	$\frac{d_n^+}{c}$	$t_n \rightarrow t_{n+1}$
$h_n^{\varphi-}(\ell,t')$	$\frac{1}{s_n^-}$	$\frac{d_n^-}{c}$	$t_{n-1} \rightarrow t_n$

By using Table 3, Eq. (52) can be arranged as

$$h_n^{\varphi\pm}(\ell,t') = C_1 \frac{dR}{\chi\sqrt{(t')^2 - \left(d_n^{\pm}\right)^2}}; \quad R_n \lessgtr ct' \lessgtr R_{n\pm1} \tag{53}$$

$V_n^{\varphi}(\ell, t_p - t_i)$ expression in Eq. (29) was given as

$$V_n^{\varphi}(\ell, t_p - t_i) = \int_{-\infty}^{\infty} T_i(t_p - t') h_n^{\varphi\pm}(\ell, t') dt' \tag{54}$$

By substituting Eq. (42), Eq. (54) can be written as

$$\begin{aligned} V_n^{\varphi}(\ell, t_p - t_i) \; = \; & \int_{\frac{R_n}{c}}^{\frac{R_{n+1}}{c}} (e(t')^2 + ft' + g) \left[\frac{C_1}{\sqrt{(t')^2 - C_2^2}}\right] dt' \\ & + \int_{\frac{R_{n-1}}{c}}^{\frac{R_n}{c}} (e(t')^2 + ft' + g) \left[\frac{C_1}{\sqrt{(t')^2 - C_2^2}}\right] dt' \end{aligned} \tag{55}$$

$V_n^{\varphi}(\ell, t_p - t_i)$ can be found in a similar way which $\psi_{m,p}$ was calculated in Section 5.2 as

$$V_n^{\varphi}(\ell, t_p - t_i) = C_1 \left[\begin{array}{l} e\left(\frac{t'\sqrt{(t')^2 - C_2^2}}{2} + \frac{C_2^2}{2} \ln\left(t' + \sqrt{(t')^2 - C_2^2}\right)\right)\Big|_a^b \\ +f\left(\sqrt{(t')^2 - C_2^2}\right)\Big|_a^b + g\left(\ln\left(t' + \sqrt{(t')^2 - C_2^2}\right)\right)\Big|_a^b \end{array} \right]$$

$$+C_1\left[\begin{array}{l} e\left(\dfrac{t'\sqrt{(t')^2-C_2^2}}{2}+\dfrac{C_2^2}{2}\ln\left(t'+\sqrt{(t')^2-C_2^2}\right)\right)\Big|_a^b \\ +f\left(\sqrt{(t')^2-C_2^2}\right)\Big|_a^b+g\left(\ln\left(t'+\sqrt{(t')^2-C_2^2}\right)\right)\Big|_a^b \end{array}\right] \tag{56}$$

In Eq. (29), $Z^{\varphi}_{mn,p-i}$ expression can be calculated as

$$Z^{\varphi}_{mn,p-i}=c^2\int\limits_{S_m}[\nabla\cdot\boldsymbol{f}_m(\ell)]V^{\varphi}_n(\ell,t_p-t_i)d\ell \tag{57}$$

Here, integration can be calculated numerically as in Section 3. $\varphi_{m,p}$ term in Eq. (29) can be written in the matrix form as

$$\varphi_{m,p}=\frac{\mu}{4\pi}\sum_{n=1}^{N}\sum_i I_{n,i}Z^{\varphi}_{mn,p-i} \tag{58}$$

6. NUMERICAL RESULTS

6.1. A Small Dipole

Usually, the Gaussian pulse is the most popular excitation used for the computation of transient responses of objects. It is wanted to be of finite duration in time and also band-limited in the frequency-domain. Gaussian plane waves which can be seen from Figure 4 can be defined mathematically as

$$\boldsymbol{E}^i(\boldsymbol{r},t)=\hat{\boldsymbol{p}}\cos(2\pi f_0\tau)\exp\left[-\frac{(\tau-t_d)^2}{2\sigma^2}\right] \tag{59}$$

where $f_0=50\,\text{MHz}$ is the center frequency, $\tau=t-\boldsymbol{r}\cdot\hat{\boldsymbol{k}}/c$ is retarded time, $\hat{\boldsymbol{k}}=\hat{\boldsymbol{x}}$ is the propagation direction, $\hat{\boldsymbol{p}}=\hat{\boldsymbol{z}}$ is the polarization, $\sigma=6/(2\pi f_{bw})$, $f_{bw}=23.87\,\text{MHz}$ is bandwidth of the signal, $t_d=3.5\sigma$. The straight thin wire structure has been used for the perfect conductor body which is shown in the Fig. 3, where the wire radius $a=1\,\text{mm}$, it is located on z axis $-1\le z\le 1\,\text{m}$ and divided into 8 equal subsections.

When the wire structure which is shown in Figure 3 is illuminated by the electric field defined in Eq. (59), the induced current in its middle point is shown in logarithmic scale in Figure 5. As seen in the figure, instability is observed starting from the initial time steps. To correct the instability, the B-MOT formulation was used. As shown in

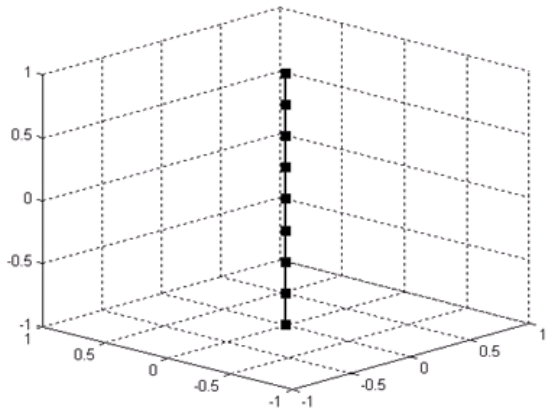

Figure 3. Straight thin wire structure.

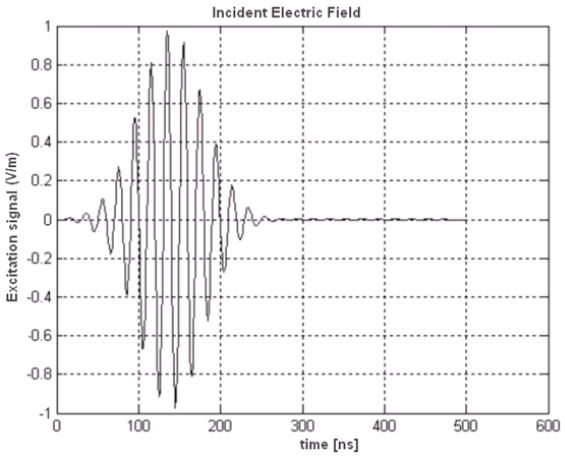

Figure 4. Incident electric field.

Figure 6, the instability observed in the time steps after 450 ns in the classic method was corrected through the Newmark-Beta formulation.

It is observed that the stability increases when β value is equal to 0.25, as seen from the Figure 7. However, it was concluded that the results are not coherent with the results produced by employing the time domain moment method given in [2]. In order to obtain better results, the A-MOT formulation was added. Figure 8 indicates that the results found by using the A-MOT are more stable than those found by using the B-MOT, while Figure 9 indicates that the results produced by using the A-MOT are more accurate and stable than those

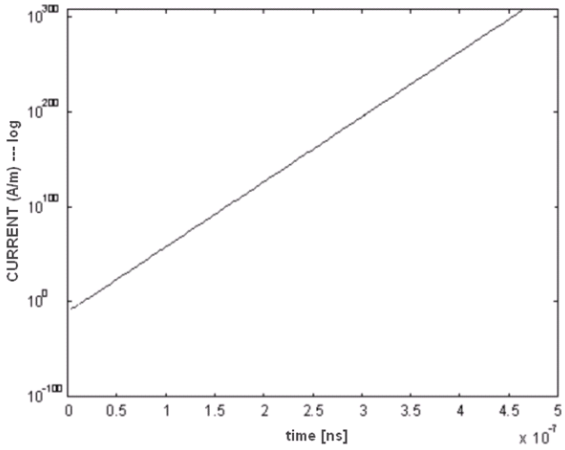

Figure 5. Induced current in thin wire's middle point (log).

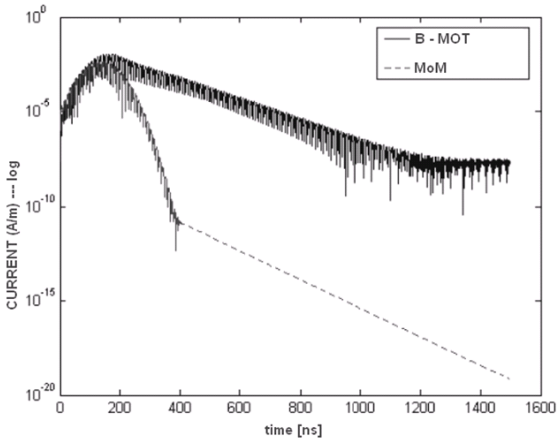

Figure 6. Comparison of MoM solution and B-MOT solution for thin wire structure.

produced by employing the time domain moment method and as seen from the Figure 10, A-MOT formulation produces stable results even $\beta = 0.2$. This can be explained as, in A-MOT formulation integrals are calculated by analytically, so resolution of matrix increased.

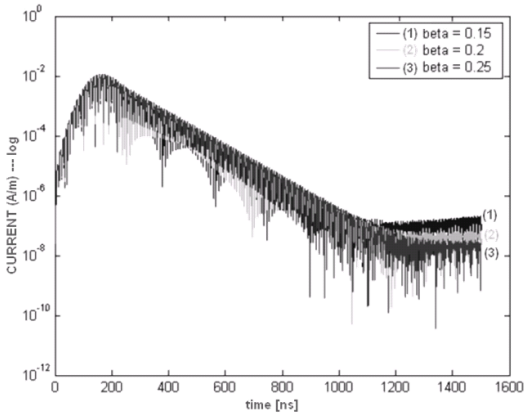

Figure 7. Current distribution calculated by B-MOT on thin wire's middle point (log) for the values $\beta = 0.15,\ b = 0.20$ and $\beta = 0.25$.

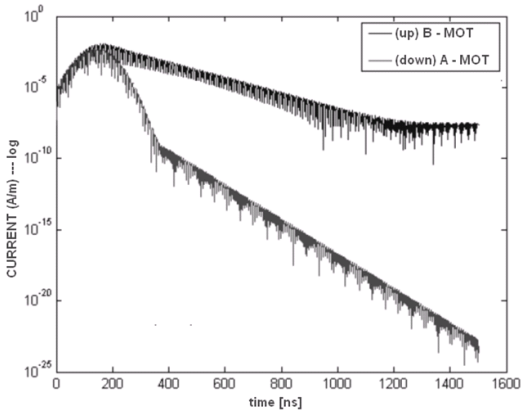

Figure 8. Comparison of the current calculated by using the B-MOT and the current calculated by using A-MOT for straight thin wire structures.

6.2. Loop Antenna

Gaussian pulse which can be seen from the Figure 11 is represented by

$$\boldsymbol{E}^i(\boldsymbol{r},t) = \boldsymbol{E}_0 \frac{4}{T\sqrt{\pi}} e^{-\gamma^2} \tag{60}$$

where $\gamma = (4/T)(ct - ct_o - \boldsymbol{r}\cdot\boldsymbol{k})$, c is the velocity of light, $\boldsymbol{k}$ is the wave vector for the incident wave, t is the time variable, T is the width of the pulse and choosen as $T = 4$, ct_o is the time delay at which the

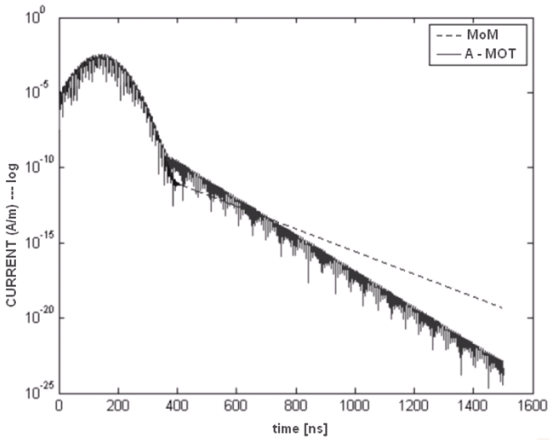

Figure 9. Comparison of MoM solution and A-MOT solution for straight thin wire structure.

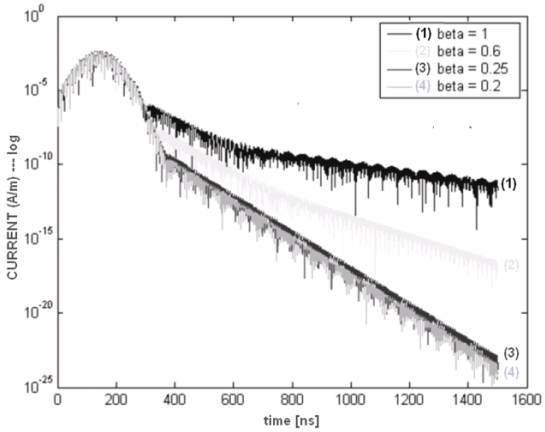

Figure 10. Current distribution calculated by A-MOT on thin wire's middle point (log) for the values $\beta = 1$, $\beta = 0.6$, $\beta = 0.25$ and $\beta = 0.2$.

pulse reaches its peak and choosen as $ct_o = 6$. Both of these quantities are defined in light meters (LM), which is the time taken by light to traverse 1 m. Figure 12 shows a loop antenna whose radius is 0.5 m [3]. Wire radius is chosen as 5 milimeter (mm) and the same gaussian pulse is used as incident field which is described in [3] and given in Eq. (60). Figure 13 shows the current distrubution which is calculated by B-MOT on point (0.5,0). The results are exactly same with [3].

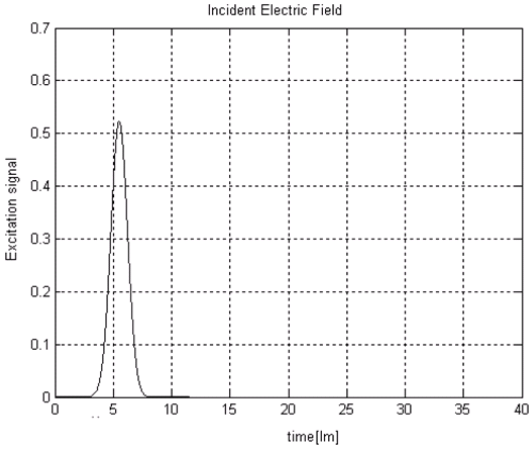

Figure 11. Incident electric field.

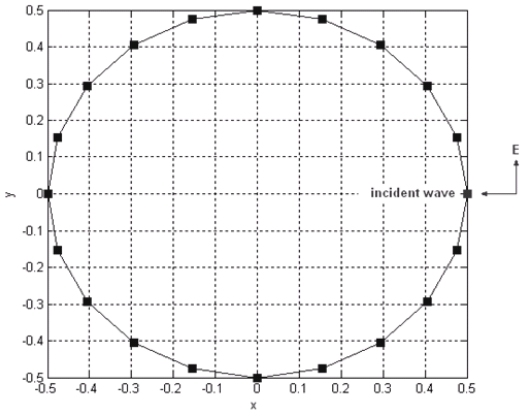

Figure 12. Loop antenna.

6.3. Three-Pole Structure

The modulated plane wave is used in [4] can be given as

$$\boldsymbol{E}^i(\boldsymbol{r},t) = \frac{4}{T\sqrt{\pi}}\boldsymbol{E}_0 e^{-\gamma^2}\cos\left[2\pi f_0\left(t - t_0 - \frac{\boldsymbol{r}\cdot\hat{\boldsymbol{k}}}{c}\right)\right] \tag{61}$$

where

$$\gamma = \frac{4c}{T}\left(t - t_0 - \frac{\boldsymbol{r}\cdot\hat{\boldsymbol{k}}}{c}\right) \tag{62}$$

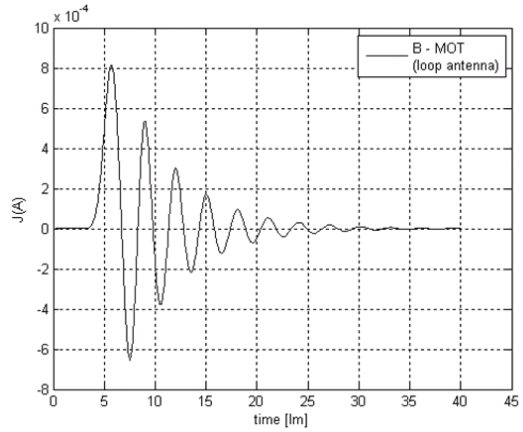

Figure 13. Current distribution calculated by B-MOT for loop antenna on the point (0.5,0).

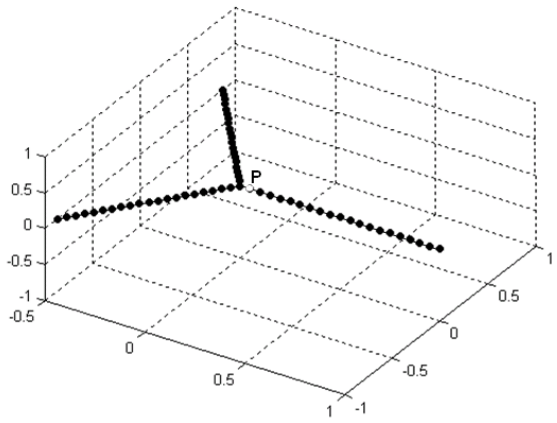

Figure 14. Three pole structure.

With $\boldsymbol{E}_0$ linked to the maximum amplitude of the incident field, T is the time length of the impulse expressed in light metres (LM), t_0 is the delay time of the incident pulse from the start of the simulation, $\hat{\boldsymbol{k}}$ is a unit vector, indicating the incidence direction of the wave, and $\boldsymbol{r}$ is the point where the field is computed. Following parameters are used: $E_0 = 120\hat{\boldsymbol{x}},\ T = 2\,\mathrm{LM},\ t_0 = 3\,\mathrm{LM},\ \hat{k} = -\hat{z},\ f_0 = 0$. The length of the three arms is 1 m, separated by 120°, each arm is divided into 20 subsections, and the wire radius is 3 mm. The three pole structure is given in Figure 14. The results obtained by B-MOT compared with [4] and it is observed that they are exactly same. B-MOT results can be seen from Figure 15.

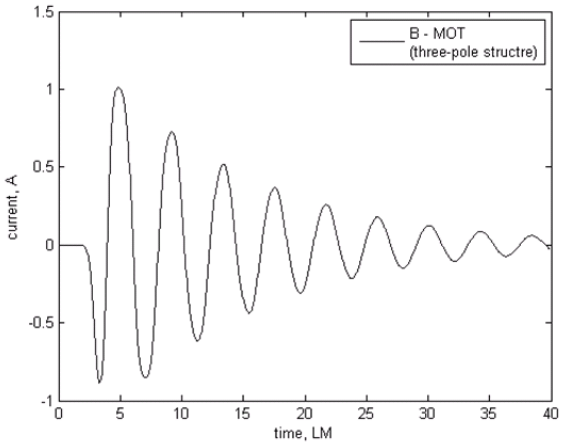

Figure 15. Current distribution on the point "*P*" for three pole structure calculated by B-MOT.

REFERENCES

1. Shanker, B., A. A. Ergin, K. Aygün, and E. Michielssen, "Analysis of transient electromagnetic scattering from closed surfaces using a combined field integral equation," *IEEE Trans. Antennas Propagat.*, Vol. 48, No. 7, 1064–1074, 2000.
2. Özsoy, Ş., "İnce tellerden oluşan yapılardan saçılma analizi için zamana ve frekansa bağlıki çözücü," Gebze Institute of Technology, 2003.
3. Ji, Z., T. K. Sarkar, B. H. Jung, Y. S. Chung, M. Salazar-Palma, and M. Yuan, "A stable solution of time domain electric field integral equation for thin-wire antennas using the Laguerre polynomials," *IEEE Trans. Antennas Propagat.*, Vol. 52, 2641–2649, 2004.
4. Guarnieri, G., S. Selleri, G. Pelosi, C. Dedeban, and C. Pichot, "Innovative basis and weight functions for wire junctions in time domain moment method," *IEE Proc. - Microw. Antennas Propag.*, Vol. 153, 61–66, 2006.
5. Taflove, A., *Computational Electrodynamics: The Finite-Difference Time-Domain Method*, Artech House, Boston, MA, 1996.
6. Rao, S. M. and D. R. Wilton, "Transient scattering by conducting surfaces of arbitrary shape," *IEEE Trans.*, Vol. 39, 56–61, 1991.
7. Vechinski, D. A. and S. M. Rao, "A stable procedure to calculate

the transient cattering by conducting surfaces of arbitrary shape," *IEEE Trans. Antennas Propagat.*, Vol. 40, 661–665, 1992.

8. Rynne, B. P. and P. D. Smith, "Stability of time marching algorithms for the electric field integral equation," *J. Electromagn. Waves Appl.*, Vol. 4, 1181–1205, Dec. 1990.
9. Sadigh, A. and E. Arvas, "Treating the instability in matching-on-in-time method from a different perspective," *IEEE Trans.*, Vol. AP-41, Dec. 1993.
10. Smith, P. D., "Instabilities in time marching methods for scattering: Cause and rectification," *Electromagn.*, Vol. 10, 439–451, 1990.
11. Hu, J. L., Chi H. Chan, and Y. Xu, "A new temporal basis function for the time-domain integral equation method," *IEEE Microwave and Wireless Communications*, Vol. 11, No. 11, Nov. 2001.
12. Wang, Y. and T. Itoh, "Envelope-Finite-Element (EVFE) technique a more efficient time-domain scheme," *IEEE Transactions on Microwave Theory and Techniques*, Vol. 49, 2241–2247, 2001.
13. Manara, G., A. Monorchio, and R. Reggiannini, "A space-time discretization criterion for a stable time-marching solution of the electric field integral equation," *IEEE Trans. Antennas Propagat.*, Vol. 45, 527–532, 1997.
14. Harrington, R. F., *Field Computation by Moment Methods*, IEEE Press, New York, 1993.